

Study on load test of 100m cross-reinforced deck type concrete box arch bridge

Jing Xian SHI¹, Ying Jie CHENG²

¹Oxbridge College, Kunming University of Science and Technology, KunMing 650106 Yunnan, China;

²Yunnan Aerospace Engineering Geophysical Detecting Co.Ltd, Kunming 650217, Yunnan, China

Abstract: Found in the routine quality inspection of highway bridge that many vertical fractures on the main beam (10mT beam) of the steel reinforced concrete arch bridge near the hydropower station. In order to grasp the bearing capacity of this bridge under working conditions with cracks, the static load and dynamic load test of box arch bridge are carried out. The Midas civil theory is calculated by using the special plate trailer - 300 as the calculation load, and the deflection and stress of the critical section are tested by the equivalent cloth load in the test vehicle. The pulsation test, obstacles and no obstacle driving test were carried out. Experimental results show that the bridge under the condition of the test loads is in safe condition, main bearing component of the strength and stiffness meet the design requirements, the crack width does not increase, in the process of loading bridge overall work performance is good.

1 Introduction

Arch bridge as an application example of arch structure, also become one of the longest bridge in the history of mankind, its light structure, beautiful shape, has the strong compression capability, widely used in highway construction, especially in the mountainous area in Yunnan province.

This article analyzes the object on the secondary highway of a mountain in Yunnan province. On the highway bridge during commissioning acceptance, routine inspection found in the 10m T beam bridge upper structure, there are more vertical cracks, especially the second and ninth on arch, the bridge in the case of fracture of carrying capacity should be further identified. The bridge load test is the most effective and direct method to understand the performance parameters of the

bridge and analyze its working condition. In order to study the carrying capacity of this bridge, load test includes static load should be used.

2 Engineering Overview

The structure of the bridge is the upper bearing reinforced concrete box arch bridge (figure 1), and the main arch ring consists of 6 arch boxes, the arch axis coefficient is 2.1, the vector ratio is 1/5. The main span is 100 meters, the vertical column and the guide hole are the steel reinforced concrete T beam with an average span of 10m, and the two-lane two-way driving. Auto load level for highway-II; The calculation load is special plate trailer -300; Seismic fortification for the VII; The peak acceleration was 0.10 g.



Figure 1 Panorama of bridge

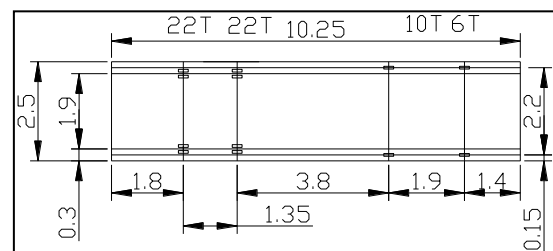


Figure 2 Loading planar size of the vehicle(unit/m)

*Corresponding author: Email: sara_shivip@163.com mail: 532965722@qq.com

The prefabricated arch, the current roof and the arch are all C40 concrete. The precast T-beam, the frame and the wall of the arch, the wall of the arch, the bridge pier, the cover girder is C30 concrete; The base class adopts C25 concrete. The diameter of reinforcement is greater than or equal to 12 mm, and HRB335 is adopted.

3 Load test pattern

According to the principle of internal force equivalent, the internal force of the structure under the action of the test load should be equal or close to the internal force of the structure under the design load. The strain (stress) and deflection of the control cross section under test load are analyzed, and the results of the test are compared with the calculation results.

3.1 Static test

In order to meet the requirements of bridge bearing capacity test, there are five working conditions of the most adverse stress state of bridge structure were selected. Respectively are: working condition1-load test of maximum pressure stress in the top section of the

main arch; working condition2-load test of the maximum compressive resistance in the cross section of the 9th midspan of T beam; working condition3---load test of the maximum compressive resistance in the cross section of the 11th midspan of T beam; working condition4-1#load test of the maximum axial force of the frame section; working condition5-9#load test of the maximum axial force of the frame section. The loading vehicle calculation diagram is shown in figure 2.

The deformation measurement points are arranged on the deck, with a total of 4 sections (figure3) and 3 points of each section (figure 4). At the corresponding points of the bridge, the height mark nails are set, and the relative elevation of the various working conditions is tested by the water level, and the deformation (displacement) of the structure is determined.

The strain tests in five control sections are shown in figure 6. The lateral arrangement is shown in figure 5, 7 and 8, and the triangle symbol in figure 7 is the dynamic strain point. The static strain test system is used to test the resistance strain gauge. The static strain test system is used to test each cross section with resistance strain gauge.

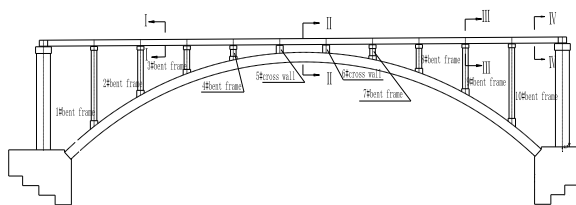


Figure 3 Vertical layout of of deformation measuring points

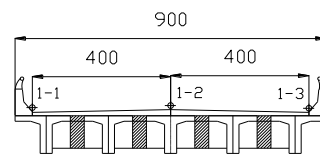


Figure 4 Deformation measuring point of 1-1 section

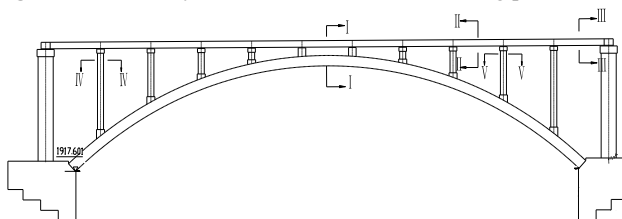


Figure 6 Vertical layout of Strain test points

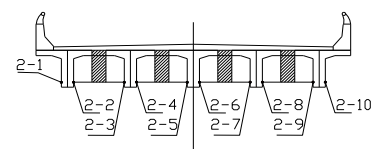


Figure 5 Strain test points of II - II section

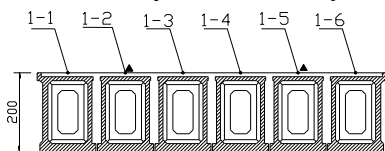


Figure 7 Strain test points of 1-1 section

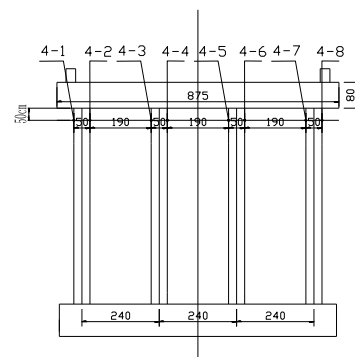


Figure 8 Strain test points of IV-IV section

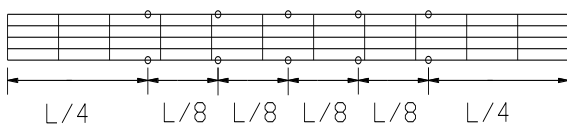


Figure 9 Measuring points of pulsating test

3.2 Dynamic test

3.2.1 Pulsating test

The vibration frequency, vibration mode and damping ratio are the inherent characteristics of the bridge, which

*Corresponding author: Email: sara_shivip@163.com mail: 532965722@qq.com

are related to the span, structure and material of the bridge. The self-vibration characteristics of the bridge structure are obtained through the pulsation experiment (the heavy vehicle excitation is adopted when necessary). The pulsation test point is arranged on the deck (figure 9) to test the acceleration of the free vibration of the bridge.

3.2.2 Barrier-free driving test

Barrier-free driving test, for testing: the dynamic response of the bridge structure under the load of the moving vehicle when the bridge deck pavement is in perfect condition, then simulate normal driving condition, using one 30 tons truck and on 5, 10, 20, 30, 40 km/h speed commute through the bridge, measuring the dynamic response of the bridge, the bridge test and calculate the actual impact coefficient.

3.2.3 Obstacles driving test

Simulating the condition of local damage of deck pavement, the dynamic response of bridge span structure under the action of moving vehicle load. The simulated obstacle height is about 5 - 10cm, with 1 30 ton trucks passing through the bridge at the speed of 5km/h.

By using the bridge structure analysis software Midas Civil, the static dynamic calculation model of the bridge space is established (only the test span is modeled and calculated). According to the regulations of the bridge design, considering the actual bridge operation load and calculate the indicators in the design criterion. The calculation results provide a reference basis for the detailed plan of the load test.

The finite element calculation model is shown in Figure 10. The contents and results of the theoretical calculation are follows:

1) Calculate the load efficiency factor based on test load (test internal force / design internal force). According to the influence line to determine the test load size and position to ensure that the load efficiency coefficient is within 0.85 ~ 1.05 range.

The working conditions: 1-1~1-3 measuring point load test efficiency were 0.97, 1.01, 1.01; condition 2: 2-1~2-3 measuring point load test efficiency were 0.87, 0.91, 0.88; condition 3: 3-1~4-3 measuring point load test efficiency were 0.88, 0.98, 0.93; condition 4: 4-1 and 4-2 condition measuring point load test efficiency were 0.86, 0.88 and condition 5: 5-1, 5-2 condition measuring point load test efficiency were 0.87, 0.85.

2) Calculate the magnitude of each experiment result under the test loading, including stress, strain and displacement. The loading deformation at working condition 1-3 is shown in figure 11.

4 Theoretical calculation

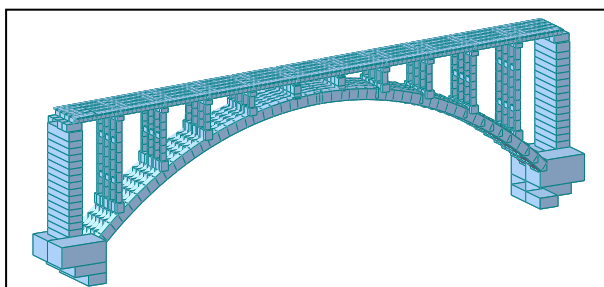
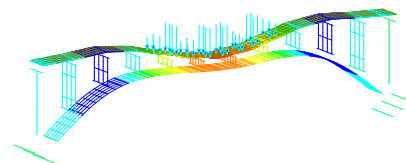
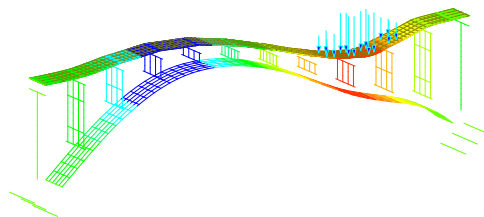


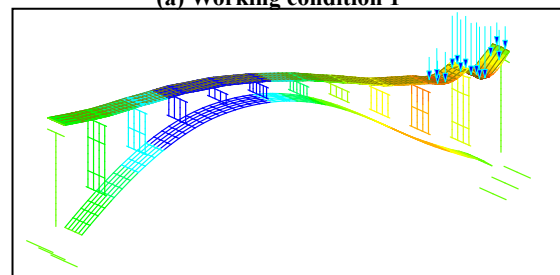
Figure 10 computing model



(a) Working condition 1



(b) Working condition 2



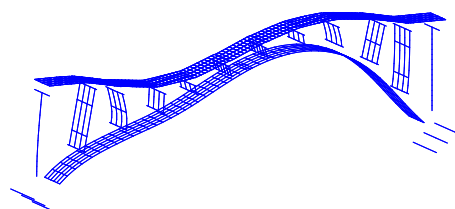
(c) Working condition 3

Figure 11 loading graph

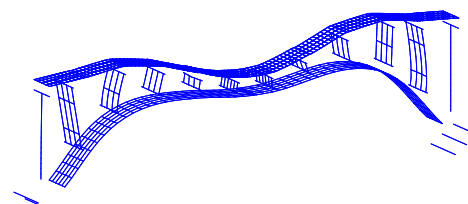
3) Dynamic calculation results

The first 5 orders of frequencies are 1.800 HZ, 2.695

HZ, 4.841 HZ, 5.121 HZ and 5.750 HZ, respectively. The first and second modes are shown in the figure 12.



(a) First-order mode



(b) Second-order mode

Figure 12 Modal measured vibration diagram

5 The results of static test

5.1 Deformation test result and testing coefficients

The deformation test results of working condition 1-5 and the residual deformation after unloading are shown in Figure 13. The data in each cross section are disturbed and the points that the instrument can not collect are eliminated.

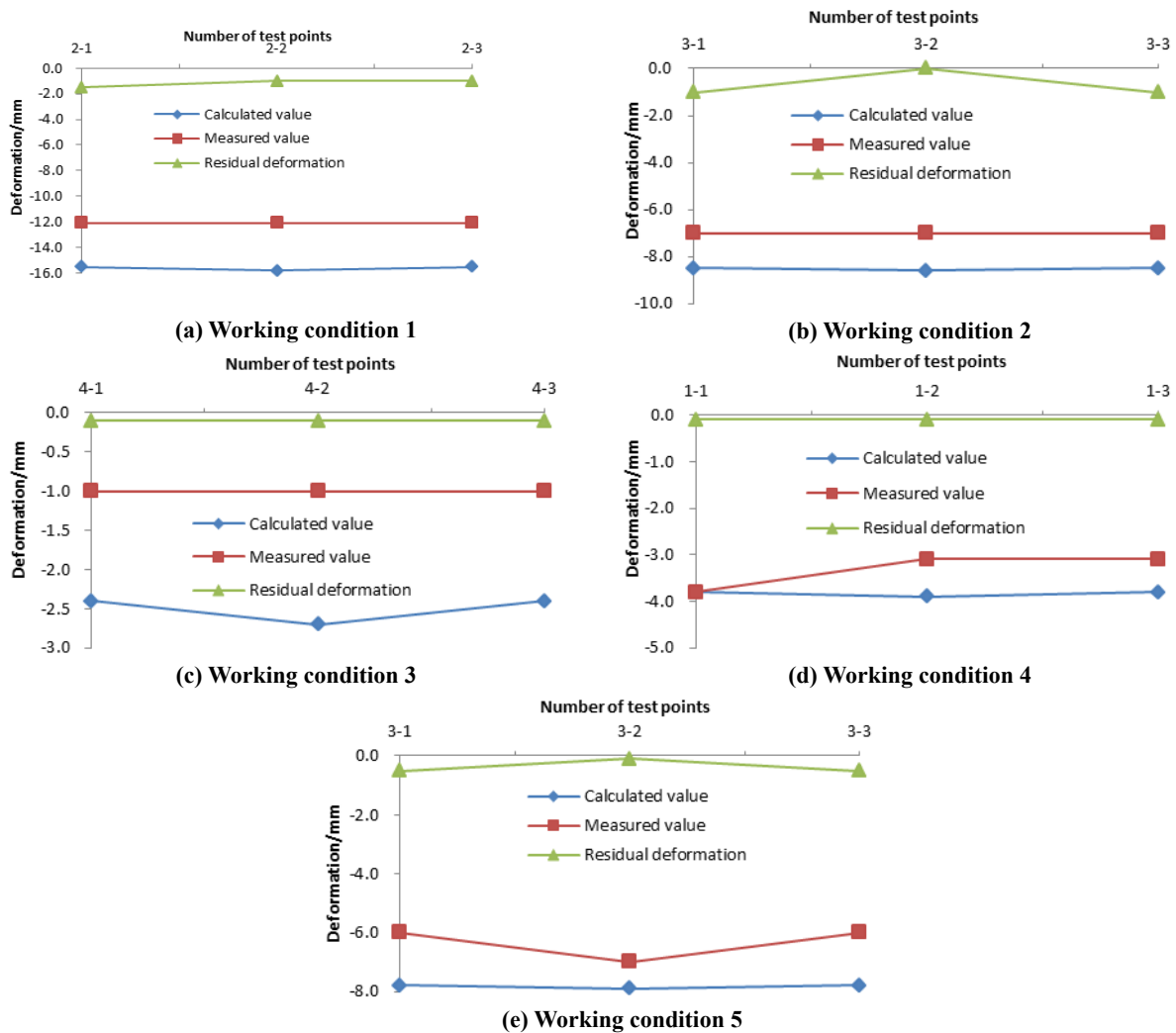
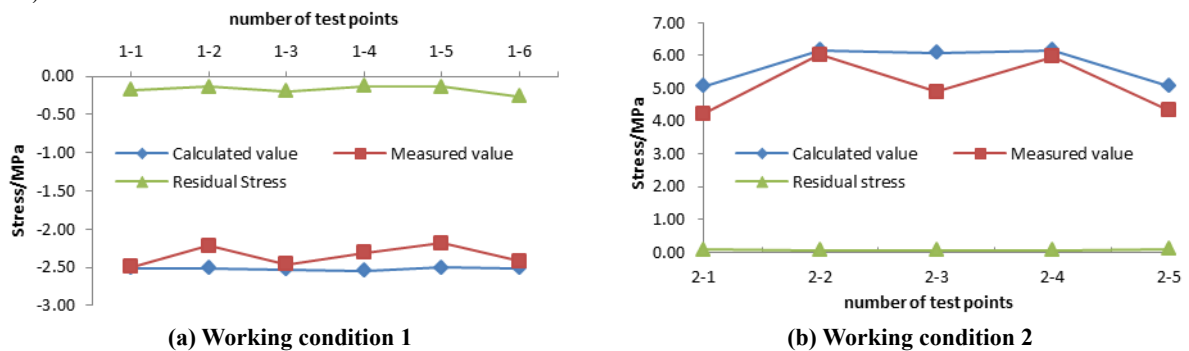


Figure 13 Deformation test results

5.2 Stress test and calibration coefficients

The stress condition of 1-5 (the measured strain is converted) test results and the residual strain after

unloading values are shown in Figure 14, it can be show that the calculated values and test values, the residual stress value after unloading is between 1%-11% (the standard limit value is 20%)



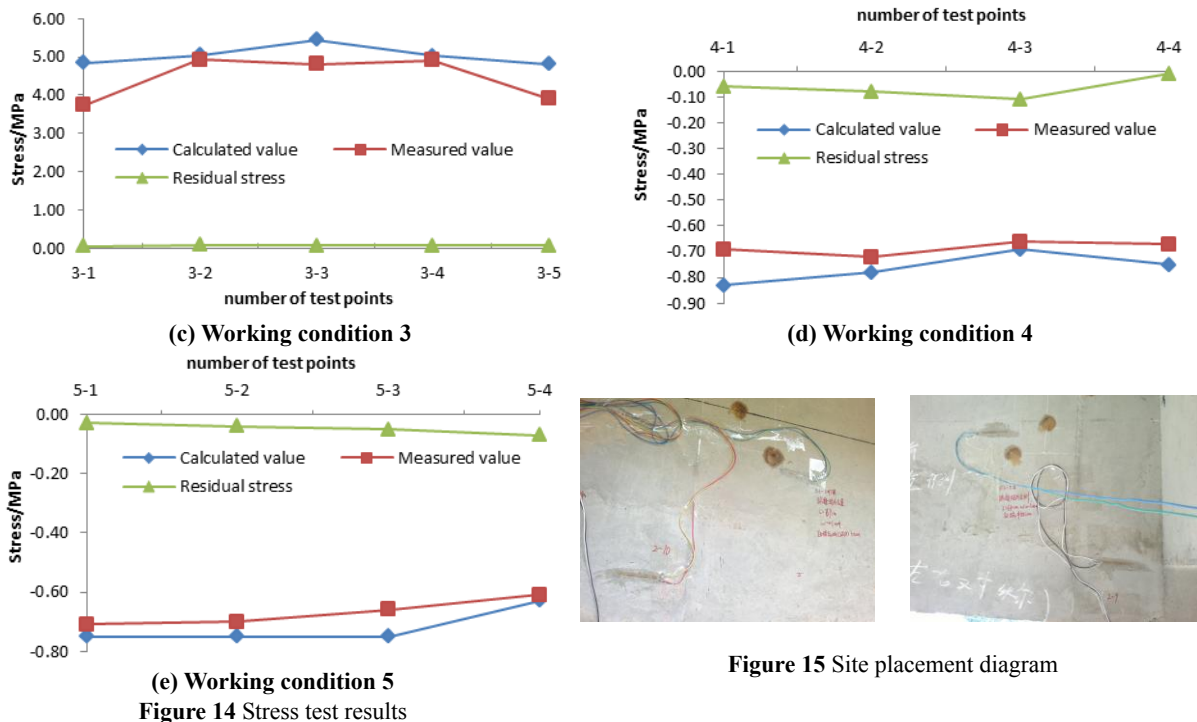


Figure 15 Site placement diagram

Table 1 Calibration coefficients of each test position

Position	Calibration coefficient	Position	Calibration coefficient	Position	Calibration coefficient	Position	Calibration coefficient	Position	Calibration coefficient
1-1	0.99	1-6	0.96	2-5	0.86	3-5	0.81	5-1	0.95
1-2	0.88	2-1	0.84	3-1	0.77	4-1	0.83	5-2	0.93
1-3	0.97	2-2	0.98	3-2	0.98	4-2	0.92	5-3	0.88
1-4	0.91	2-3	0.80	3-3	0.88	4-3	0.96	5-4	0.97
1-5	0.87	2-4	0.97	3-4	0.98	4-4	0.89		

5.3 Fracture stress test results

During the load test, the cracks observation point was arranged in the T beam of sixth and eleventh span of the main arch. In the crack position, the cross-seam patch is

carried out (figure 15). The crack position is located on the second test section and third test section, Beam3-3, Beam3-5, Beam5-2, Beam5-5 left and right sides. The position diagram of the patch is shown in figure 15 and the test results is shown in table 2.

Table 2 Test results of crack deformation

Measuring position	Crack initial width/mm	Increased crack width/mm	Whether to return to zero after unloading	Measuring position	Crack initial width/mm	Increased crack width/mm	Whether to return to zero after unloading
Beam3-3-L	0.1mm	0.063	return to zero	Beam5-2-L	0.1mm	0.056	return to zero
Beam3-3-R	0.1mm	0.060	return to zero	Beam5-2-R	0.13mm	0.055	return to zero
Beam3-5-L	0.15mm	0.064	return to zero	Beam5-5-L	0.1mm	0.054	return to zero
Beam3-5-R	0.05mm	0.030	return to zero	Beam5-5-R	0.13mm	0.053	return to zero

Note: 3-3- L indicates the direction of the road forward, third spans, third T beams, and left side of the beam.

6 The results of Dynamic test

6.1 Free - vibration characteristic test

The modal shapes are shown in Figure 16. After the data analysis and processing, the fundamental frequency of the structural free - vibration is obtained, the measured values and theoretical values are shown in table 3.

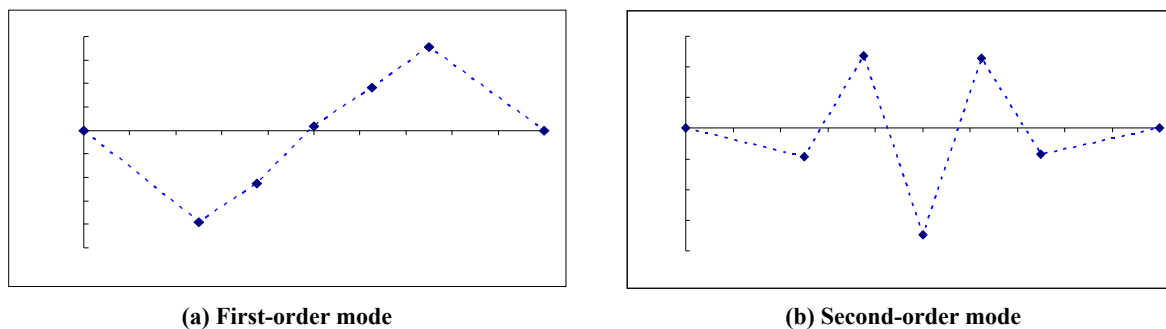


Figure 16 Modal measured vibration diagram

Table 3 Natural frequency and damping test value

Measured order	Test value (Hz)	Calculated value (Hz)	ζ	Main vibration direction
First order	1.981	1.800	0.018	Vertical bending
Second order	2.854	2.695	0.015	Vertical bending

6.2 Impact coefficient test results

Through test, the typical dynamic response curve at different speed is tested. After processing the data, the

impact coefficient of the bridge at different speed is shown in table 4 (The design specification calculates $1+\mu = 1.23$).

Table 4 Test value of impact coefficient

Measuring point	Speed/km/h	Maximum stress/MPa	Impact coefficient	Measuring point	Speed/km/h	Maximum stress/MPa	Impact coefficient
Dynamic strain measuring point 1 (1-2)	5	2.33	----	Dynamic strain measuring point 2 (1-5)	5	2.26	----
	10	2.38	1.018		10	2.29	1.010
	20	2.37	1.014		20	2.30	1.014
	30	2.38	1.018		30	2.31	1.018
	40	2.40	1.027		40	2.31	1.020
5(Vehicle bumping)	2.47	1.058	5(Vehicle bumping)	2.42	1.071		

7 Conclusion

The test vehicle is conducted on the equivalent load according to the design load, and the results of static and dynamic tests show that the bridge has a good bearing capacity, and the bridge is in a safe state under the test load condition.

1) The strain and deformation of the bridge under the static load conditions show that the bridge is under the design load and is in the elastic working stage. After unloading, the zeroing condition is normal and no new cracks occur, which proves the strength of the main load-bearing members of the bridge meets the design requirements.

2) The test stress calibration factor of the bridge under static load is between 0.85~1.01, The measured maximum displacement is 12mm (less than the design limit), It shows that the bridge structure and materials meet the design requirements and the overall performance is good.

3) The bridge dynamic test results show that the first vertical free-vibration frequency is 1.981Hz, the damping

ratio is 0.018, the impact coefficient is 1.010-1.071, the test mode and the theoretical modal shows good agreement and stiffness of bridge structure meets the design.

References

1. Wang Hai-peng, Study on the Bearing Capacity Estimation of Deck Type Concrete Box Arch Bridge Based on Load Test [J], CONSTRUCTION TECHNOLOGY, 2015(09):33-35.
2. HU Yong, TAN Dong-lian. Large-Tonnage Static Load Test and Simulation Analysis on the Approach Way Bridge of a Hydropower Station [J]. Research & Explore. 2010(07).
3. Shuang Yang Zhang, Qian Hui Pu, Ren Da Zhao, Zhou Shi. Load Test Design and Stability Analysis of Basket Handle Arch Bridge with Reinforced Concrete [J]. Advanced Materials Research, 2014, 2837(838).
4. Christopher D. Moen, Elaine E. Shapiro, Julia Hart. Structural Analysis and Load Test of a

- Nineteenth-Century Iron Bowstring Arch-Truss Bridge[J]. Journal of Bridge Engineering,2013,18(3).
5. Devin K. Harris, John M. Civitillo, Amir Gheitasi. Performance and Behavior of Hybrid Composite Beam Bridge in Virginia: Live Load Testing[J]. Journal of Bridge Engineering,2016.
 6. Łukasz Filar, Jerzy Kałuża, Marek Wazowski. Bridge Load Tests in Poland Today and Tomorrow – The Standard and the New Ways in Measuring and Research to Ensure Transport Safety[J]. Procedia Engineering,2017,192
 7. Shervan Ataei, Meysam Jahangiri Alikamar, Vahid Kazemiashtiani. Evaluation of Axle Load Increasing on a Monumental Masonry Arch Bridge Based on Field Load Testing[J]. Construction and Building Materials,2016.
 8. JTG/T J21-2011, Specification for Inspection and Evaluation of Load-bearing Capacity of Highway Bridges [S].
 9. JTG / T J21-01-2015, Load Test Methods for Highway Bridges [S].
 10. WU Xiao-guang, BAI Qing-xia, LEI Zi-xue. Application Calculation Example of Specifications for Strengthening Design of Highway Bridges [M]. Beijing: China Communications Press, 2011.